An Improved Numerical Scheme to Treat the Open Lateral Boundary of a Regional Model

YOSHIO KURIHARA, CHRISTOPHER L. KERR* AND MORRIS A. BENDER

Geophysical Fluid Dynamics Laboratory/NOAA, Princeton University, Princeton, New Jersey

(Manuscript received 27 February 1989, in final form 22 June 1989)

ABSTRACT

A numerical scheme proposed by Kurihara and Bender is modified so as to improve the behavior of open lateral boundaries of a regional model. In the new scheme, both the local values and the gradients of fields from a larger model are used to define the time-dependent reference values toward which the boundary gridpoint values of the regional model prediction are relaxed at each step of the model integration. Use of the gradients in the boundary forcing imposes constraints on the vorticity, divergence and baroclinicity fields for the regional model. The relaxation time of forcing is set to be short for the normal component of wind. For other variables, the relaxation time at a given boundary gridpoint depends on the wind direction at that gridpoint, with a minimum at a point of normal inflow and a maximum at a point of normal outflow. The forcing strength is reduced in the planetary boundary layer so that the boundary layer structure is determined mainly by the surface condition of the regional model. Also, a simple method to control the total mass in the regional model is described. Numerical results from 96-hour integrations with the improved scheme are compared with those from the previous scheme for the cases of the propagations of a wave and a vortex. The behavior of the model at the lateral boundary was noticeably improved with the use of the new scheme, while the solution in the interior domain was little affected by the scheme modification.

1. Introduction

To carry out numerical integrations of a regional model in a one-way mode, time-dependent lateral boundary conditions derived from the earlier time integration of a larger model usually of a coarser resolution are customarily imposed. The latter model will be called a host model in this paper. One-way mode integration is often required for reasons of computational economy. It may also be useful when the physics of a regional model is not fully compatible with that of a host model. An important presumption or expectation is that the prediction with the host model is reasonably accurate.

It is desirable that the fields near the lateral boundary of the regional model are kept close to those of the host model during the time integration and that they smoothly connect to the solutions in the interior domain. Kurihara and Bender (1983, hereafter referred to as KB) proposed a scheme which met the above conditions fairly well. Their scheme consists of three procedures: 1) the prediction at boundary gridpoints with the use of the open-side conditions which are obtained without host model data; 2) the relaxation of the predicted winds at boundary gridpoints toward the time-dependent reference winds which are prescribed from the host model integration; also the computation of temperatures at boundary gridpoints through the thermal wind relation; and 3) the smoothing of the momentum field within a six-point boundary zone by a method of Newtonian-type damping. In the formulation of their scheme, they assumed that the high frequency modes were well suppressed in the regional model and did not prevail near the lateral boundary. Then, the propagation direction of a quantity across the boundary was determined from the normal component of wind at each boundary gridpoint. With the use of the propagation direction thus defined, they imposed a stable boundary condition in forcing the reference wind to the boundary value. The mass field was computed so that the balance was maintained with the wind field at the boundary gridpoints.

In the present study, we again assume that the wind vector at a boundary gridpoint can closely approximate the propagation direction of a quantity. However, if the predominant modes passing across the lateral boundary of the regional model are the fast modes, the above assumption does not hold and a boundary scheme which is suitable for treating these modes has to be used instead.

The KB scheme has been used successfully in many numerical simulation experiments of tropical cyclones performed at the Geophysical Fluid Dynamics Laboratory, NOAA. In general, the behavior of wind and mass fields near the lateral boundary were acceptable. In one case, Typhoon Roger moved out from the re-

* Present affiliation: Cray Research, Inc.

Corresponding author address: Dr. Yoshio Kurihara, GFDL/NOAA, Princeton University, P.O. Box 308, Princeton, NJ 08542.

gional model domain in agreement with its actual movement (Tuleya 1988). However, we noticed the existence sometimes of small scale noise or somewhat large gradients in certain fields in the boundary zone. The sources of these computationally generated irregularities should be removed or suppressed as much as possible. This has been accomplished in this study without changing the fundamental framework of the KB scheme.

Another problem we have encountered in using the KB scheme is an unrealistic gradual increase or decrease of the total mass in the regional model, i.e., the area integrated surface pressure. Although the total mass of a regional model should be allowed to change, it has to be maintained within a reasonable range. The total mass could be controlled by small adjustment, on order of a few centimeters per second, of the normal component of wind along the boundary during the time integration. We will propose another feasible method to overcome this annoying problem.

In section 2, we list various problem areas for which the improvement of the KB scheme were considered. In section 3, we present the best design that we have found through evaluation of a large number of schemes. Examples of the performance of the proposed scheme are given in section 4, and concluding remarks are made in section 5.

2. Problem areas

In order to improve the open lateral boundary condition, various ideas were examined through time integrations of a limited area 11-layer primitive equation model for the two cases described below. During the integration, the information from a host model was required. In the present study, we defined beforehand the states of the host model for the period of 96 hours.

a. Case 1: A propagating Haurwitz wave (zonal wavenumber 10) in a moist atmosphere

The regional model covered a domain of 45 degrees longitude by 37 degrees latitude with 1 degree resolution. The model physics and the initial condition are basically the same as those of Case 2 in KB. The state of the host model was taken from the solution for the nondivergent barotropic case. Namely, it was obtained by shifting the initial state westward at a known constant angular velocity. Note that the physics of the regional model is different from that of the host model.

b. Case 2: A vortex moving on a stationary Haurwitz wave (zonal wavenumber 8)

The structure of the regional model was the same as that for Case 1. The initial condition was established by embedding a vortex on a stationary Haurwitz wave in the similar manner as done by Bender and Kurihara (1987) in their numerical study. The vortex, which did not extend to the lateral boundary at the initial time, was expected to be steered by the wave toward the eastern boundary and eventually move out of the model domain. On the other hand, we presumed that the host model could not resolve the vortex. Accordingly, the two models were different from each other, not only in the physics, but also in the initial conditions.

Numerical results from the time integrations for the above two cases, together with our experiences with the use of the KB scheme, suggested that we could better treat the open lateral boundary of a regional model by paying attention to the following problems.

(i) Open side condition. Open side conditions have been used in KB for making predictions at a boundary gridpoint, i.e., at the center of a boundary grid box. To obtain the temperature at the open side of a boundary grid box, the condition of geostrophic balance was used in KB. For generality, this condition needs to be modified to that of the gradient wind balance. When the mixing ratio of the water vapor at the open side was computed by a linear extrapolation scheme, it sometimes caused too high or too low a relative humidity at the open side. This needs to be rectified.

(ii) Definition of reference states. We relax the predicted values at boundary gridpoints toward appropriately defined reference values. When a host model is not entirely consistent with the regional model, setting the reference values equal to the values of the host model could impose too much of a constraint on the regional model. Sometimes this resulted in an increase in the magnitude of the wind divergence near the boundary and an increase in the accumulated amount of precipitation. A strong horizontal shear could also develop near the boundary. The moving vortex in Case 2 became distorted as it approached the boundary. Also, the unrealistic gradients that sometimes developed in the temperature and mixing ratio fields near the boundary contributed to the appearance of various undesirable features.

It seems reasonable to constrain the boundary of a regional model not only with the local values but also with the gradients of fields from the host model. We propose to combine these two constraints in defining reference values. Results of test integrations showed that many problems encountered before could be suppressed significantly by such an approach. The above two constraints may be compared to the Dirichlet and the Neumann conditions for treating partial differential equations of elliptic type.

In our scheme, the relaxation of predicted values toward reference values is made only at boundary gridpoints. We examined a number of methods in which the forcing was applied in relaxation regions of several grid widths. This type of scheme using a relaxation region has been used by Davies (1976) and others. The numerical results we obtained with such methods were not superior to the results with our new scheme as far as Cases 1 and 2 of the present study were concerned.

In many instances, an erroneous flow, though very weak, developed in relaxation regions apparently due to small imbalance between the wind and mass in the forced fields. Such an imbalance was often ascribed to variation of the relaxation parameter which we expressed, as customarily done, in terms of distance from the domain boundary. We also investigated schemes in which the time tendencies of the host model was used like the one by Perkey and Kreitzberg (1976). We noticed distortion of the fields as the integration proceeded. In these schemes, boundary gridpoint values were, in effect, determined by the host model. Therefore, the difference in physics between the two models, if any, could easily cause spurious normal gradients in the fields near the boundary.

Since the forcing considered in this study is not instantaneous but of a relaxation-type, host model data at an advanced time level may be used to define reference values. A final point to note is that the vertical profiles of temperature and moisture of a host model may not be convectively stable when checked by the physics of a regional model. In such a case, the data from the host model should be adjusted to a convectively neutral state before being used for defining the reference values. The same consideration may be used in defining the initial condition of the regional model.

(iii) Strength of forcing. We have to carefully specify the strength of forcing of a reference value or, in other words, the degree of relaxation of a predicted value. An appropriately specified forcing should produce a stable integration and smooth fields with minimal distortion. We consider that the lateral boundary forcing at lower levels should be weak so that the boundary layer structure is determined largely by the physics and the surface condition of the regional model, with little influence of the host model. We propose to reduce the strength of forcing smoothly from the free atmosphere toward the surface.

As demonstrated in KB, a numerical scheme is acceptable in which the normal component of wind is constrained at all boundary gridpoints and other variables at inflow points only. (We suppose that, in a first approximation as assumed in KB, the local wind at a boundary gridpoint indicates the propagation direction of a quantity.) However, an abrupt change of constraint, from forcing on an inflow segment of the boundary to no forcing on an adjacent outflow segment, contributed sometimes to distortion of fields near the boundary. Results of our investigations clearly suggest that we can obtain much smoother fields by a scheme in which the strength of forcing varies smoothly along the domain boundary. Specifically, we propose to determine the forcing strength from the direction of local wind relative to the boundary line rather than from the direction of its normal component alone.

(iv) Suppression of noise. Small scale noise that otherwise appeared in some of the model integrations was effectively suppressed through smoothing of the Newtonian damping type described in KB. This smoothing did not produce any noticeable effect on the large scale field. It should be included in an improved scheme.

(v) Constraint on the total mass. We assume that the total mass of the regional model can deviate from that of the host model, while the surface pressure near the domain boundary should be, on the average, close to the host model surface pressure. A simple scheme satisfying the above condition is proposed in which continual correction is made to the surface pressure of the regional model. Such correction, usually quite small, should be uniformly applied to the entire domain so that it does not affect the pressure gradient force. The constraint we impose is weaker than the total mass adjustment to a host model value through matching of boundary mass fluxes.

3. Formulation of an improved scheme

In this section, an improved version of the KB scheme is described. It was formulated in accordance with suggestions made in the preceding section.

a. Open side condition

Each of the wind components, normal and tangential, at the open side of a boundary box is obtained by the linear extrapolation of the values from the interior. The surface pressure is treated in the same manner. The temperature and geopotential are derived from the relationship of dynamical balance described in KB with the addition of the inertia force term to the Coriolis force term. The mixing ratio of water vapor at the open side is estimated from the temperature at the open side and the relative humidity which is assumed to be the same as that of the boundary gridpoint.

b. The relaxation toward reference values

The problems (ii) and (iii) addressed in section 2 are all taken into account in the formulation of the following scheme.

We use the notation h_m to represent a gridpoint value of a variable h in a regional model after each marching with its dynamics and physics. We denote a corresponding reference value by h_0. The second set of subscripts, C and $C-1$, will be used to denote a boundary gridpoint and the next inner gridpoint, respectively. The forcing at the boundary gridpoint with the relaxation time t_d may be expressed as

$$\left(\frac{\partial h_m}{\partial t}\right)_C = -t_d^{-1}[h_{m,C} - h_{0,C}]. \tag{3.1}$$

Solving the implicit finite difference version of (3.1), we find the forced value at the boundary gridpoint to be

$$h_{F,C} = \frac{1}{1+A}[Ah_{m,C} + h_{0,C}] \tag{3.2}$$

where A is the relaxation parameter which measures t_d in the unit of a time increment, Δt, so that $A = t_d/\Delta t$. We need additional formulas for $h_{0,C}$ and A.

Ordinarily, data sets from a prediction with a host model are saved at an interval of several hours. We prepare hourly data by a linear time interpolation of those data in which we have removed the convective instability as judged from the criterion of the regional model physics. We let h_g denote the nearest available future hourly value thus obtained. Using hourly values is not only practical and computationally economical but also helps reduce boundary noise. The reference value is defined as

$$h_{0,C} = w[h_{m,C-1} + (h_{g,C} - h_{g,C-1})] + (1 - w)h_{g,C}. \quad (3.3)$$

Note that the two terms on the right-hand side cause forcing of the normal gradient and of the value of the host model field, respectively. The latter contributes to the forcing of the tangential gradient. Due to the involvement of the gradient forcing, the regional model value, $h_{m,C-1}$, appears in (3.3). Accordingly, in the proposed scheme, the reference value cannot be prescribed but is obtained in the course of the integration of the regional model. The weight factor w in (3.3) can take different values for different variables. In case of the momentum, we consider that constraining the vorticity and divergence, or the wind gradient, is equally as important as constraining the wind itself. On the other hand, imposing strong constraint on the gradient seems to be reasonable in case of the temperature and the moisture because the mass field affects the momentum field through its gradient. Particularly, we expect that the mass gradient and the momentum in the host model are well balanced with each other. We also note that, if the physics of the regional model is not exactly the same with that of the host model, relaxation toward the temperature and moisture values of the host model can eventually produce systematic, erroneous gradients near the boundary. Guided by the above considerations, we assign the following values to w in (3.3), with which satisfactory results were obtained in the integrations of both Case 1 and Case 2:

$w = \frac{1}{2}$ for the wind components

$w = 1$ for the temperature, mixing ratio and sea level pressure. (3.4)

In the case of the mixing ratio, if the reference value becomes less than ϵ, it is set to ϵ where $\epsilon = 10^{-20}$ in our model. As indicated in (3.4), we propose to apply the forcing to the sea level pressure rather than to the surface pressure, since the surface altitudes specified in the regional and the host models are not necessarily the same with each other. Reduction of the pressure from the surface (p_*) to the sea level (p_s), and vice versa, may be made by

$$p_s = \alpha p_* \quad (3.5)$$

where

$$\alpha = [T_{KMAX}/(T_{KMAX} + \Gamma z_*)]^{-g/(R\Gamma)}. \quad (3.6)$$

In (3.6), T_{KMAX} denotes the temperature at the lowest model level; g is the acceleration due to gravity; R is the gas constant; Γ is set equal to 6.5 K km^{-1} and z_* is the surface altitude in either the regional or host model.

We let the relaxation parameter A in (3.2) take the following form:

$$A = A_1(\theta) \cdot A_2(\sigma) \quad (3.7)$$

where the factor $A_1(\theta)$ expresses the dependency of the strength of boundary forcing on the direction of the wind vector relative to the boundary and $A_2(\sigma)$ is used to reduce the forcing strength at levels in the planetary boundary layer. The angle θ is measured counterclockwise so that θ is equal to $\pi/2$ for an outflow normal to the domain boundary and $3\pi/2$ for an inward flow normal to the domain boundary. The quantity σ is the pressure normalized by the surface value. As explained before, the parameter A is a measure of the relaxation time; a small value of A implies a short relaxation time and, hence, strong forcing, while a large value of A means a long relaxation time and weak forcing.

We impose strong forcing on the normal component of wind at all boundary gridpoints by setting $A_1(\theta)$ to an appropriate small value regardless of the angle θ:

$$A_1(\theta) = A_{\min}. \quad (3.8)$$

For the tangential component of wind, temperature and mixing ratio, we use the following formula so that the forcing strength smoothly varies along the boundary:

$$A_1(\theta) = \frac{1}{2}(A_{\max} + A_{\min}) + \frac{1}{2}(A_{\max} - A_{\min})\sin\theta. \quad (3.9)$$

The above formula is also applied to the sea level pressure with the angle θ determined for a vertically integrated wind. It is easily seen that (3.9) yields the minimum relaxation parameter $A_{\min}$, or the strongest forcing, when the wind vector at a boundary grid point is normal to the domain boundary and directed inward ($\theta = 3\pi/2$), and the maximum parameter $A_{\max}$, or the weakest forcing, when the wind vector is perpendicular to the boundary and directed outward ($\theta = \pi/2$). In practice, appropriate values for $A_{\min}$ and $A_{\max}$ may be found by experiment. In the test experiments presented in the following section, we used (3.8) and (3.9) with $A_{\min} = 20$ and $A_{\max} = 200$. A much greater value for

$A_{\min}$, i.e., weaker forcing, tended to cause the departure of regional model fields from the host model at an inflow boundary. A much smaller value for $A_{\max}$ in (3.9), i.e., too strong of a forcing at an outflow location, could excite noise because of strong overspecification of the boundary conditions. In some recent numerical experiments of hurricane simulation using real data from the NMC (National Meteorological Center) analysis, the above scheme with $A_{\min} = 5$ and $A_{\max} = 200$ yielded very satisfactory results.

The constraint on the open boundary at low levels is reduced by increasing the relaxation time. Specifically, for both the normal and tangential components of the wind, $A_2(\sigma)$ of (3.7) is defined to increase linearly from $a_{\min}$ (=1) at the assumed top level of the planetary boundary layer σ_{KTOP} (0.895 in the present study) to $a_{\max}$, which is set to 2, at the lowest model level σ_{KMAX} (0.992),

$$A_2(\sigma) = \begin{cases} a_{\min} & \text{for } 0 \leqslant \sigma \leqslant \sigma_{KTOP} \\ \dfrac{a_{\max}(\sigma - \sigma_{KTOP}) + a_{\min}(\sigma_{KMAX} - \sigma)}{\sigma_{KMAX} - \sigma_{KTOP}}, & \\ \text{for } \sigma_{KTOP} < \sigma \leqslant \sigma_{KMAX}. & \end{cases} \tag{3.10}$$

For the temperature and mixing ratio, we further reduce the strength of forcing by making $A_2(\sigma)$ larger, especially near the lowest level, because we suppose that the profiles of these quantities should be dependent mostly on the in situ surface condition of the regional model. Thus, for the temperature and mixing ratio, we define

$$A_2(\sigma) = \begin{cases} a_{\min}, & \text{for } 0 \leqslant \sigma \leqslant \sigma_{KTOP} \\ [A_2(\sigma) \text{ for the wind}] \times \dfrac{\sigma_{KMAX} - \sigma_{KTOP}}{\sigma_{KMAX} - \sigma}, & \\ \text{for } \sigma_{KTOP} < \sigma < \sigma_{KMAX}. & \end{cases} \tag{3.11}$$

For the lowest level, for which A_2 and, hence, A becomes infinite if (3.11) is applied, we set $h_{F,C} = h_{m,C}$ from (3.2). In the case of sea level pressure, we set

$$A_2(\sigma) = 1. \tag{3.12}$$

For a corner point, we determine the reference value from the average of two values that are obtained by applying (3.3) to each of the zonal and meridional directions. The definition of the relaxation parameter for each corner point is done in a similar manner by obtaining the wind direction with regard to each of two boundary lines forming a domain corner.

c. *Smoothing in the boundary zone*

After boundary gridpoint values are relaxed toward their respective reference values, possible noise in the momentum and moisture fields within a six-gridpoint boundary zone is suppressed, as suggested in problem (iv) of section 2. The smoothing scheme used is of the

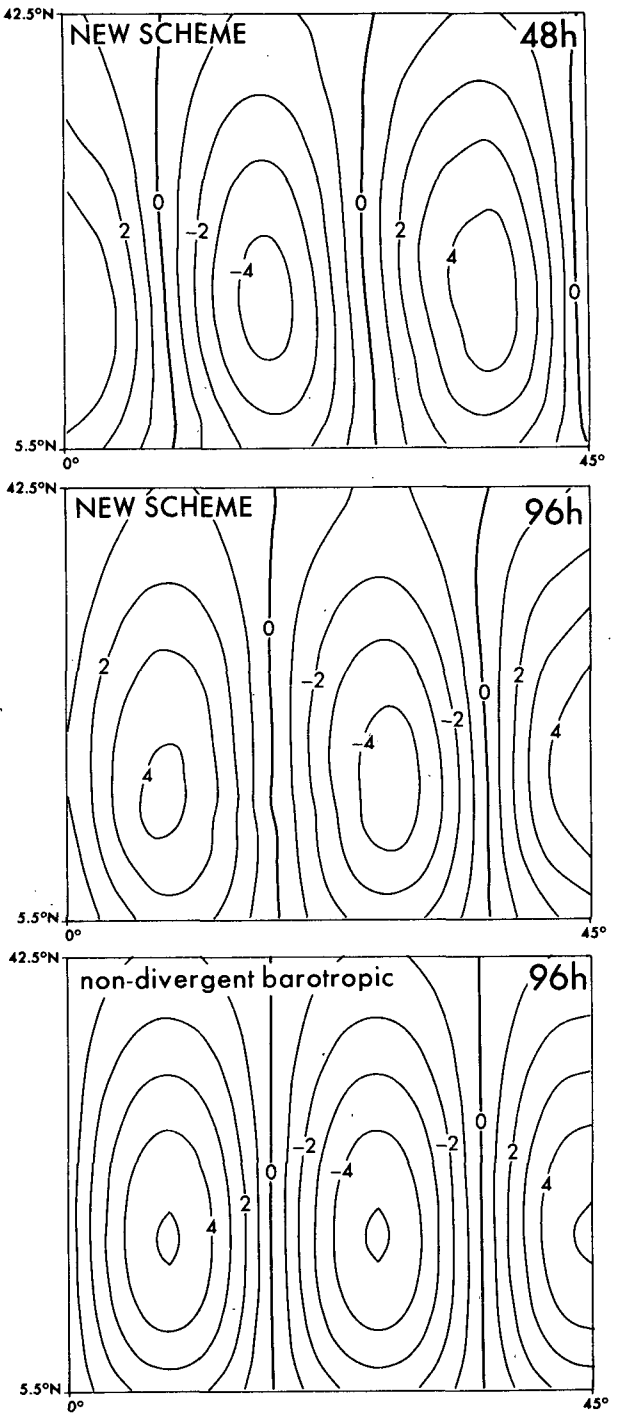

FIG. 1. The 48 h and 96 h distribution of the meridional wind (m s^{-1}) at model level 5 ($\sigma = 0.5$) using the new scheme for Case 1. For comparison, the analytic solution at 96 h for the nondivergent barotropic case is also presented at the bottom.

Newtonian damping type, which takes a form similar to (3.2). In this case, the reference values for the tangential wind component and the mixing ratio at a boundary gridpoint are obtained from the averages of the two adjacent boundary gridpoints, while that for the normal wind also involves the value at the inner gridpoint, which is weighted double in taking the average. The reference values for points on the second through sixth rows or columns from the boundary are computed for each variable from the average of values at the four surrounding gridpoints. At each corner point, the values at the two adjacent boundary points are averaged. Based on our experience, the relaxation parameter, A, is set to 40, 40, 80, 120, 180 and 240 for the first through sixth gridpoint from the boundary, respectively. The moisture field was not smoothed when the reference value was greater than the gridpoint value.

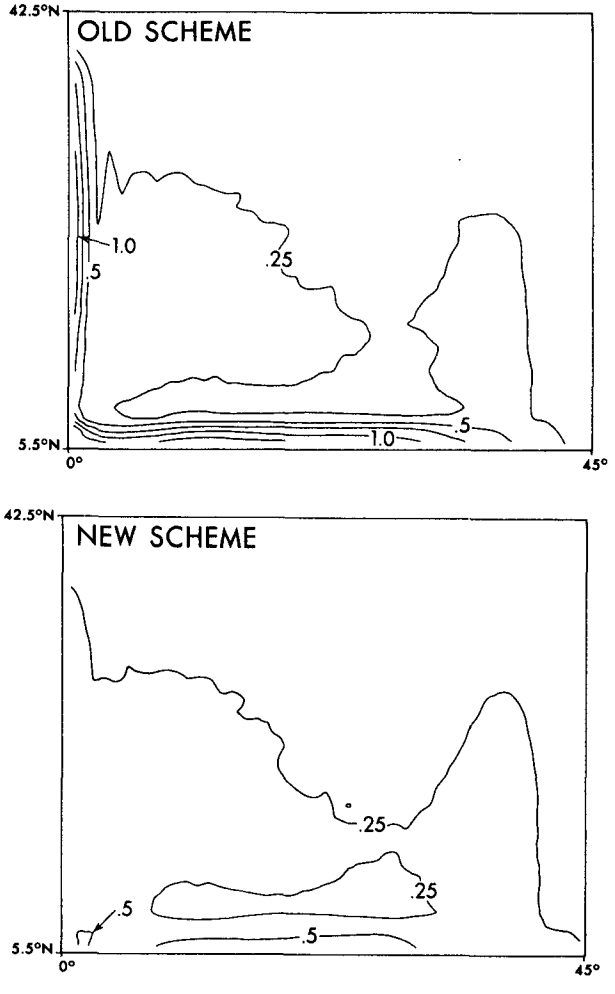

FIG. 2. Distribution of the accumulated precipitation (cm) during 96 h integration of Case 1, using the old scheme (top) and new scheme (bottom).

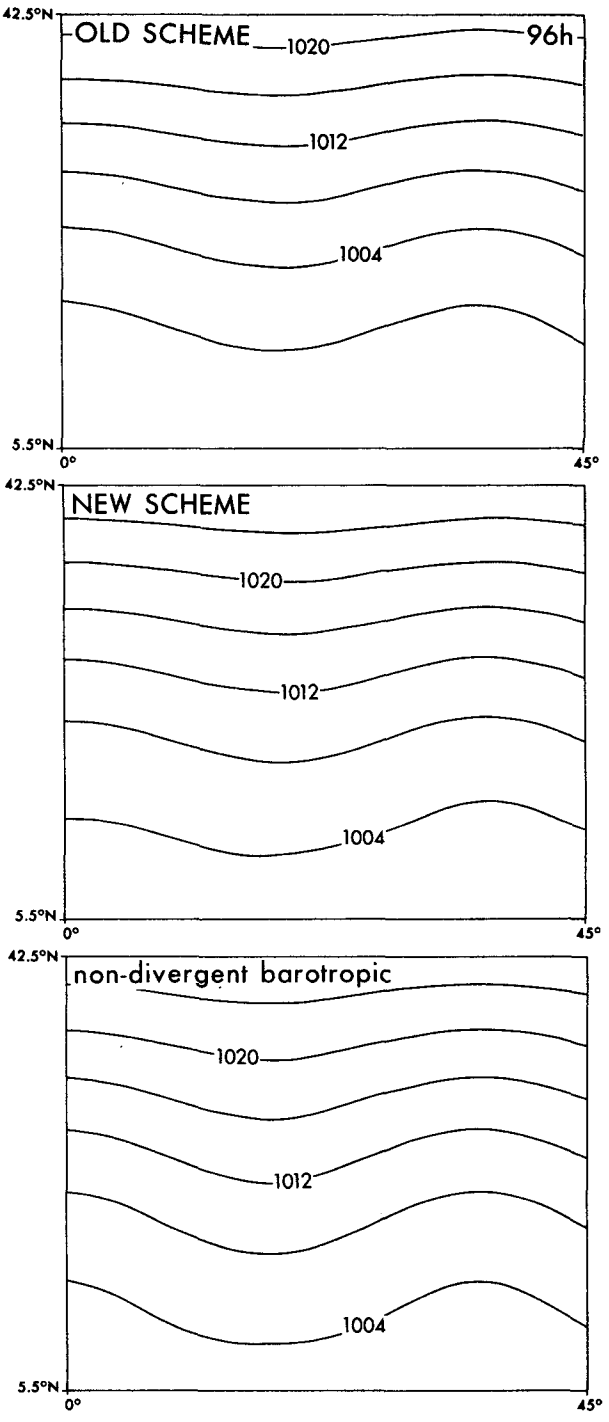

FIG. 3. Distribution of the surface pressure (mb) at 96 h for Case 1, using the old scheme (top) and new scheme (middle). For comparison the analytic solution at 96 h for the nondivergent barotropic case is also presented at the bottom.

d. Correction of the surface pressure

As discussed in problem (v) of section 2, we perform the surface pressure correction by adding a tiny time-

dependent value to the entire surface pressure field. The correction amount is simply the area average of the difference between the host model and the regional model values, $h_g - h_m$, of the sea level pressure for the narrow border zone containing all first and second gridpoints from the boundary. Owing to the use of the narrow border zone, the correction amount is little influenced by the evolution of the surface pressure field in the interior of the regional model.

4. Numerical examples

As mentioned in section 2, tests of the new boundary scheme (hereafter referred to as the New Scheme) were made by 96 hour integrations for two test cases. For comparison, test integrations were also performed with the original scheme of KB (Old Scheme). Case 1 involved the propagation of a Haurwitz wave in a moist atmosphere, while Case 2 involved a vortex moving on a stationary Haurwitz wave.

The meridional winds at 48 and 96 hours at model level 5 ($\sigma = 0.5$) are shown (Fig. 1) for Case 1, using the new scheme. The analytic solution at 96 hours for the nondivergent barotropic case is also presented at the bottom for comparison. The propagation of the wave was quite similar to the nondivergent barotropic solution. The shape of the wave was well maintained up to 96 hours, with the trough and ridge positions in good agreement with the analytic solution. At all vertical levels of the model, the values at the lateral boundary smoothly connected to the interior solutions for the fields of mass, momentum and moisture. With the use of the old scheme, differences developed between the values at the lateral boundary and the interior solution, especially at the model levels near and in the boundary layer. The degree of distortion of the fields may be measured by the mean square vertical velocity. Its value for the entire model, averaged for 72–84 hours, was 4.6 (in 10^{-9} hPa^2 s^{-2}) for the old scheme as compared with 1.4 for the new scheme.

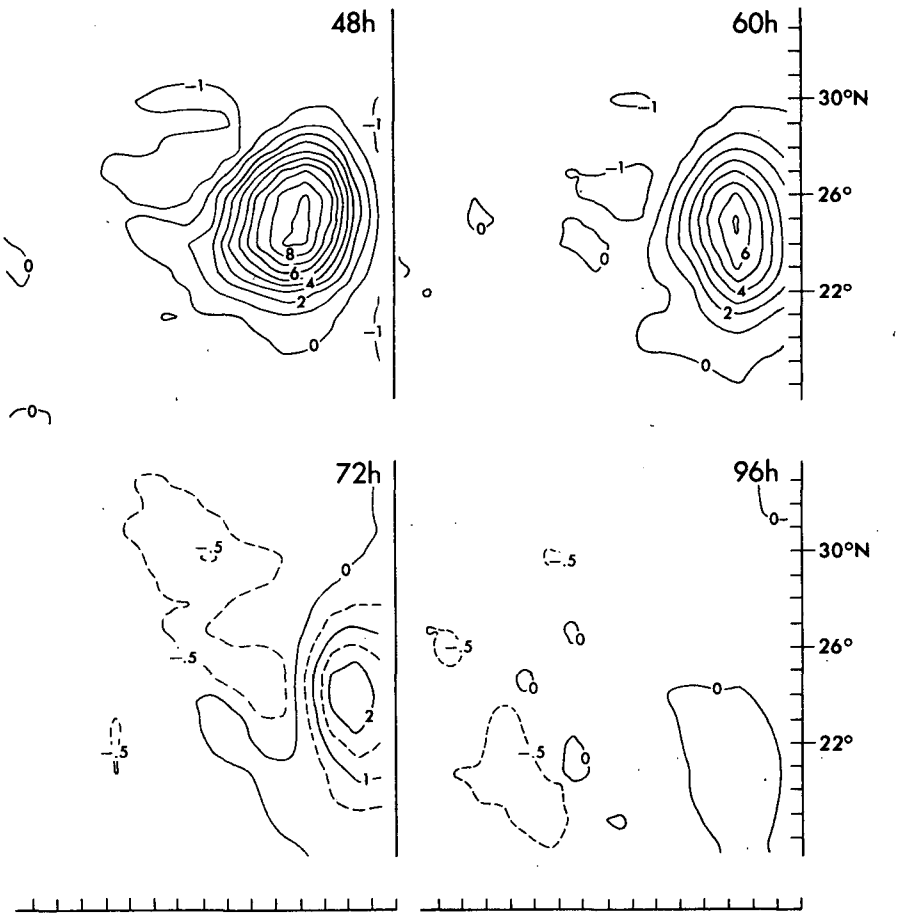

FIG. 4. Distribution of vorticity (in units of 10^{-5} s^{-1}) for Case 2 at 48, 60, 72, and 96 h at model level 7 ($\sigma = 0.8$) using the new scheme, for the eastern section of the integration domain. The tick marks at the bottom and right side indicate the 1 degree spacing of the grid points.

A related improvement due to the new scheme, compared to the old one, was found in the reduction of excessive convergence at the lateral boundary. As a result, the accumulated precipitation by the end of the integration was much reduced (Fig. 2) at the southern and western boundary. However, these differences in the boundary zone did not appear to have a significant impact on the interior solution, as suggested in Fig. 2 by the basic similarities in the interior region between the two experiments.

In Fig. 3 we see that the surface pressure correction employed in the new scheme could control the total mass quite well. In particular, the old scheme, which did not have a pressure correction, exhibited an average mass decrease of about 5.8 mb for the domain shown after 96 hours of integration, in contrast to the new scheme in which a mass change of about −0.4 mb occurred.

The results for Case 2 are presented in Figs. 4 and 5. For these figures we included only the eastern section of the total integration domain where the vortex approached the boundary. The shape of the vorticity associated with the disturbance (Fig. 4) remained well maintained as the vortex crossed the lateral boundary using the new scheme. The storm weakened as it approached the boundary, probably due, in part, to the Newtonian damping type smoothing used in the boundary zone. By 96 hours the storm successfully passed through the boundary, with no apparent noise generated within the integration domain. In contrast, the vorticity distribution associated with the storm became spread along the boundary when the old scheme was used (Fig. 5). Also, a strong southerly component in the meridional wind was produced by the old scheme at the lateral boundary as the vortex approached. But we also observe from Fig. 5 that, well inside the bound-

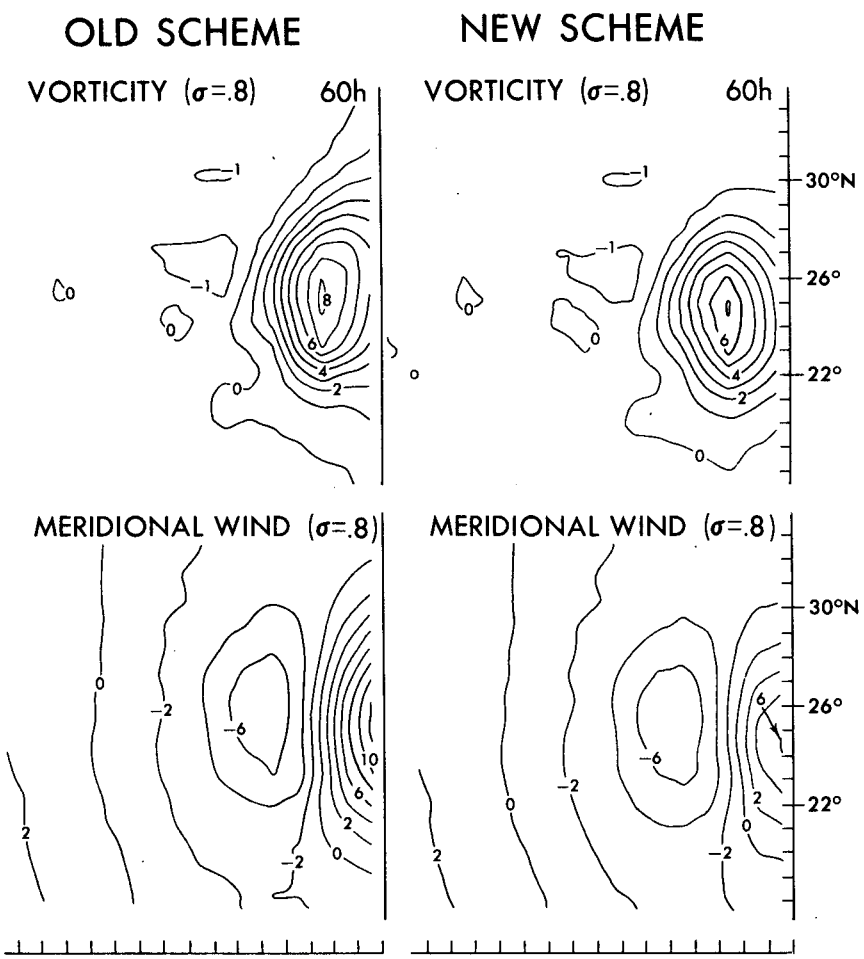

FIG. 5. Distribution at 60 h of vorticity (in units of 10^{-5} s^{-1}) and the meridional component of the wind (m s^{-1}) for Case 2 using the old scheme (left) and new scheme (right), for the eastern section of the integration domain. The tick marks at the bottom and right side indicate the 1 degree spacing of the grid points.

ary region, the distributions of both the vorticity and meridional wind were very similar for both boundary schemes. This again indicates that the solution in the interior of the domain for the present test case was not significantly affected by the choice of the two lateral boundary schemes used.

5. Concluding remarks

The behavior of a regional model near an open lateral boundary was noticeably improved by the use of the proposed new scheme as compared with that obtained with the previous scheme of KB. Two factors contribute to the improvement. First, the gradients as well as the local values of the fields of the host model are used in the definition of time-dependent reference values toward which the predicted values at boundary gridpoints are relaxed. The forcing involving the gradient can impose reasonable boundary constraints on the vorticity, divergence and baroclinicity fields of the regional model. This approach also reduces the difficulty which can result from any systematic difference in the behavior of two models. The second factor contributing to the improvement is a smooth variation of the relaxation parameter that governs the strength of boundary forcing. The parameter value depends on the direction of the local wind vector, rather than on the direction of the normal component alone. Also, the strength of forcing is gradually reduced in the planetary boundary layer as the height decreases.

We note here that the solutions in the interior domain for Cases 1 and 2 obtained from the integrations with the new improved lateral boundary conditions were remarkably similar to the results with the KB scheme, even in detailed features after a 96 hour integration. This gives strong support to the validity of the numerical results obtained previously from the model integrations using the KB scheme.

Usefulness of numerical schemes may be determined from accumulation of the actual performance record, in addition to results of designed tests such as those presented in our paper. Our new scheme has also demonstrated excellent performance in several numerical simulation experiments with the GFDL hurricane model. In these experiments using real data, the boundary conditions were imposed either in simulation (i.e., analysis) mode, in forecast mode, or in an extreme test of forcing to an initial state. In all cases treated so far, the obtained fields generally varied smoothly inward from the lateral boundary and excessive convergence did not develop near the boundary. It seems to us that the new scheme is likely to work in other models and for many different cases as well, though its actual applicability is yet to be seen.

Acknowledgments. The authors wish to thank B. Ross of GFDL and L. Kantha of the Institute for Naval Oceanography for making comments of great value on earlier versions of this paper. Thanks are also due to W. Marshall for typing the manuscript and to P. G. Tunison, K. Raphael, J. Varanyak and J. Connor for preparing the figures.

REFERENCES

Bender, M. A., and Y. Kurihara, 1987: A numerical study of the effect of the mountainous terrain of Japan on tropical cyclones. *Short- and Medium-Range Numerical Weather Prediction,* T. Matsuno, Ed., Meteorological Society of Japan, 651–663.

Davies, H. C., 1976: A lateral boundary formulation for multi-level prediction models. *Quart. J. Roy. Meteor. Soc.,* **102,** 405–418.

Kurihara, Y., and M. A. Bender, 1983: A numerical scheme to treat the open lateral boundary of a limited area model. *Mon. Wea. Rev.,* **111,** 445–454.

Perkey, D. J., and C. W. Kreitzberg, 1976: A time-dependent lateral boundary scheme for limited-area primitive equation models. *Mon. Wea. Rev.,* **104,** 744–755.

Tuleya, R. E., 1988: A numerical study of the genesis of tropical storms observed during the FGGE year. *Mon. Wea. Rev.,* **116,** 1188–1208.